Journal of Dynamics, Monitoring and Diagnostics, 2024, 3, 246-257
https://doi.org/10.37965/jdmd.2024.562

ISTP
RESEARCH ARTICLE

Industrial Battery State-of-Health Estimation with Incomplete Limited Data Toward Second-Life Applications

Shaojie Yang,[1] Long Ling,[1] Xiang Li,[2] Jintong Han,[1] and Shijie Tong[3]
[1]Department of Mechanical and Aerospace Engineering, University of California San Diego, La Jolla, CA 92093, USA
[2]Key Laboratory of Education Ministry for Modern Design and Rotor-Bearing System, Xi'an Jiaotong University, Xi'an 710049, China
[3]Smartville Inc., Carlsbad, CA 92011, USA

(Received 30 May 2024; Revised 07 July 2024; Accepted 30 July 2024; Published online 30 July 2024)

Abstract: Battery state-of-health (SOH) estimation is vital across applications ranging from portable electronics to electric vehicles, particularly in second-life applications where accurate prediction becomes complex due to varying degradation levels. This paper introduces a novel SOH estimation model to address the lack of labeled data, employing domain-adversarial neural networks (DANNs) combined with one-dimensional convolutional neural networks (CNNs). The proposed method allows for effective transfer of knowledge between diverse battery conditions, enhancing adaptability and efficiency by utilizing both source and target datasets. Experimental results demonstrate that the proposed model achieves a mean absolute error (MAE) of 1.68% and a root mean squared error (RMSE) of 2.50%, with minimal data. Specifically, the model requires only one cell of unlabeled data from the second-life target domain, utilizing only the dQ/dV curve for estimation. Proposed model sets a new standard in second-life battery health monitoring and management by effectively leveraging a minimal amount of data for training, and this approach offers a robust solution for accurate SOH estimation, particularly in scenarios with limited access to labeled data.

Keywords: battery degradation; deep learning; lithium-ion battery (LIB); second life; SOH estimation

I. INTRODUCTION

Lithium-ion batteries (LIBs) are pivotal in modern energy storage solutions, powering a wide range of applications from consumer electronics to electric vehicles (EVs) and large-scale energy storage systems. As global production and adoption of EVs surge, the retirement rate of these vehicles also increases, leading to an urgent need to repurpose their batteries for second-life applications before considering recycling [1–3]. This demand emphasizes the importance of effective battery management, especially as these batteries often operate beyond their prime, with capacities reduced to below 80% of their original state. When LIBs in EVs reach 80% of their initial capacity, they are retired from vehicular use and begin their second life, often in less demanding applications such as stationary energy storage systems [4]. This transition from high-performance mobility applications to stationary applications poses unique challenges in battery management due to the varied degradation and operational histories of the batteries.

LIBs are complex systems, requiring continuous monitoring to ensure their reliability and safety [5–8]. Key parameters such as voltage, temperature, state-of-charge (SOC), state-of-health (SOH), and remaining useful life (RUL) are essential for effective battery management. While voltage and temperature can be directly measured through sensors, SOC, SOH, and RUL cannot be measured directly and must be estimated [9,10]. A critical aspect of battery management systems is the accurate estimation of the SOH, which reflects the current condition of the battery relative to its ideal state.

The accurate estimation of SOH is of importance to users for several reasons. First, it ensures the safe operation of the battery by preventing overcharging or deep discharging, which can lead to hazardous situations such as thermal runaway. Second, it optimizes the batter's performance by enabling efficient energy management, thereby extending the battery's lifespan and reducing maintenance costs. Third, precise SOH estimation is critical for predicting RUL, which helps in planning maintenance and replacement schedules, thus minimizing downtime and enhancing the overall reliability of the system. Therefore, SOH estimation is a major concern for both manufacturers and users, driving the need for robust and reliable estimation methods. The degradation characteristics of LIBs can vary widely depending on the battery chemistry. In some cases, batteries that have similar degradation profiles during their first life might exhibit more pronounced or entirely different degradation behaviors once they are repurposed for second-life applications. For instance, nickel-manganese-cobalt (NMC) and lithium-iron-phosphate (LFP) batteries might show relatively stable performance declines in their first life but could have varied degradation trajectories post the 80% capacity threshold [11]. This is due to the accumulated effects of microstructural changes, electrolyte decomposition, and electrode surface transformations that have progressed differently based on initial usage conditions, charging protocols, and environmental factors [12]. All these factors making SOH estimation particularly challenging, as it demands models that can capture the multifaceted nature of battery aging [13].

Corresponding author: Xiang Li (e-mail: lixiang@xjtu.edu.cn).

Significant studies have been devoted to predicting battery SOH in recent years [14–18]. They result in the two main paradigms: model-based and data-driven methods. Mode-based methods rely on mathematical and physical models to represent the underlying processes and mechanisms within the battery [19]. For example, Feng *et al.* [20] developed an equivalent-circuit model to capture the chemical and physical relationships with the implementation of system identification algorithms, and it can identify the correlated parameters of battery behavior and degradation. Model-based methods attempt to mitigate domain shift by incorporating parameters that capture variations in operating conditions, battery chemistry, and usage patterns. By using these parameters as adjustable inputs, model-based techniques can be tuned to accommodate different domains [21]. While these models can provide detailed insights, they are typically computationally intense and may not be practical for real-world applications.

In comparison with model-based methods, data-driven methods leverage statistical and machine learning algorithms to identify patterns and relationships within empirical data [22–24]. These methods offer the advantages of being adaptable, scalable, and less dependent on the complex internal dynamics of batteries. Recent advancements in machine learning and data analytics have significantly enhanced the capability of data-driven models to accurately predict battery SOH [25,26]. Existing data-driven methods include convolutional neural networks (CNNs), long short-term memory (LSTM), Gaussian process regression (GPR), and so on [27]. By utilizing various types of data such as voltage, current, temperature, and charge/discharge cycles, these models can capture the patterns and trends associated with battery degradation. However, one of the primary challenges in utilizing these methods is the requirement for large amounts of labeled data, which can be difficult and expensive to obtain. Furthermore, models trained on data from a specific battery type or operating condition often perform poorly when applied to different batteries or conditions due to domain shifts. This requirement is particularly problematic for batteries in second-life applications, where variability in the source and history of the batteries introduces additional complexity. Second-life batteries, often sourced from different types of vehicles and used under varied conditions, exhibit diverse degradation patterns.

Data-driven methods address domain shift through techniques like feature normalization, domain adaptation, and Grassmann manifold [28–31]. Techniques like domain adaptation offer a solution to the data scarcity challenge by allowing models trained on well-documented, homogeneous datasets to be effectively adapted to less characterized, heterogeneous second-life battery data [32,33]. In the context of battery SOH estimation, this means leveraging knowledge from readily available datasets, possibly from different battery chemistries or operational conditions, to make accurate predictions on new and less-documented SOH ranges. This approach not only mitigates the need for extensive labeled data in every specific application but also enhances the model's adaptability and efficiency [34–39]. While these techniques have yielded valuable insights and advancements in SOH prediction, they are not without limitations. Lu *et al.* [35] introduced a method utilizing a swarm of deep neural network methods for estimating battery SOH. However, this model requires the use of thousands of battery samples for training and is limited to an SOH range of 100%–75%. Zhang *et al.* [39] developed a soft-dynamic time warping domain adaptation network for cross-domain SOH estimation. However, the study focused on batteries with identical chemistry and SOH range, differing only in their operational conditions. Challenges arise from the complexity and variability of battery chemistry, the diverse range of SOH, and the unique characteristics of individual applications. These factors often constrain the generalization capabilities of traditional domain adaptation methods, leaving room for improvement in predictive accuracy and adaptability.

In real-world second-life applications of LIBs, it is often the case that only sufficient data from the source domain are available, with incomplete and unlabeled data from the target domain, which may encompass different battery health levels (SOH), various operational conditions, and other distinct characteristics. This complex challenge in second-life energy storage systems has received little attention and is not well addressed in the literature. For instance, Gotz's study demonstrated fast prediction capabilities but was limited to a single battery cell used for both training and testing, which compromises the robustness of the findings [40]. Similarly, Braco's work on reused Nissan Leaf EV modules, which estimated SOH ranging from 91.3% to 31%, did not disclose the volume of data used for training, thereby questioning the reliability of the performance if insufficient data is provided [41]. Furthermore, Faraji-Niri's approach involved electrochemical impedance spectroscopy combined with machine learning to estimate SOH for second-life batteries, but it only targeted batteries with SOH ranges from 100% to 80%, thus not fully addressing the typical conditions of second-life batteries [42].

Despite the research of various data-driven techniques, no study has comprehensively addressed the simultaneous challenges of different battery chemistries, diverse operational environments, limited data, and varying SOH ranges of estimating SOH for retired LIBs from EVs. To address this issue, we have proposed a deep learning-based transfer learning methodology. The following are the key novelties and contributions of this research:

1) The SOH estimation problem is investigated by utilizing unlabeled battery data from second-life target domain, where only a segment of the SOH ranges from a single battery cell within the target domain's life cycle is employed during the training stage.
2) The differential capacity (dQ/dV) curve analysis is introduced to extract features that directly reflect the battery's health status. This method is effective in addressing the variations in battery chemistry and operational conditions, providing a comprehensive understanding of degradation patterns across different domains.
3) CNNs and domain-adversarial neural networks (DANNs) are deployed to ensure robust model performance. These neural networks are crucial for accommodating the uncertainties and variability within the datasets, leading to more precise and reliable SOH estimations.

To validate the effectiveness of our methodology, we conducted experiments on second-life battery cells, as no public dataset targets SOH levels exceeding 80%. These experiments test the model's ability to predict SOH ranges beyond first-life applications, demonstrating the practical applicability and scalability of our approach.

The reminder of this paper is organized as follows. Section II gives the problem statement, datasets, methodology overview, and the proposed SOH estimation model. Section III discusses the experimental results and performance evaluation. Finally, Section IV concludes the paper and outlines potential future research directions.

II. MATERIALS AND METHODS

The research methodology shown in Fig. 1. outlines a framework designed to improve the prediction accuracy for battery SOH estimation using domain adaptation. We utilize a strategy involving both source and target domains. This approach comprises two main components: offline training and online monitoring. In the offline training phase, the deep neural network is first pretrained using sufficient aging data from the source domain Ds. This pretraining process helps in initializing the network parameters based on the abundant labeled data available in the source domain. Once the network parameters are initialized, both the source domain data Ds and the target domain data Dt are fed into the network. During this phase, the deep neural network is trained to adapt the feature distributions between the source and target domains. This adaptation process aims to generalize the model to perform well on both the source and target domains. By aligning the feature distributions, the network learns domain-invariant features that are crucial for accurate SOH estimation across different domains. After the model has been trained and the parameters have been optimized to minimize domain discrepancy, it is deployed for online monitoring for the target domain data. In this stage, the trained model is used to predict the SOH of the target domain batteries in real time. The model leverages the knowledge transferred from the source domain to provide accurate and reliable SOH estimations, even with the limited labeled data available in the target domain.

A. DATASET INTRODUCTION

The focus of this study is on the estimation of the SOH of batteries under conditions where data may be insufficient or unlabeled. To demonstrate the application of domain adaptation in second-life SOH modeling, experiments have been conducted using Nissan Leaf retired batteries. As shown in Fig. 2, the experimental setup has eight battery modules that each include two battery cells, an ITECH battery tester for charging and discharging the batteries. The aging cycles were conducted in alignment with energy storage market applications. The batteries were charged and discharged according to a 7-day schedule, following both day-ahead and real-time energy timing shifts. During the testing, key parameters of the battery such as voltage, current, and temperature were recorded. After every four aging tests, a characteristic test which includes complete low current charge and discharge was performed. The coulomb counting method, also known as the ampere-hour integral method, was applied to compute the batteries' capacities. The overall number of testing cycles ranges from 1500 to 2100.

For validation of our approach, we utilized the MIT battery dataset from Severson's group [43] as source domain, which consists of 124 commercial high-power LFP/graphite A123 APR18650M1A cells subjected to similar fast-charging tests using a 48-channel Arbin LBT battery testing cycler. All tests are conducted under a constant environmental temperature of 30 Celsius. Each test is programmed with

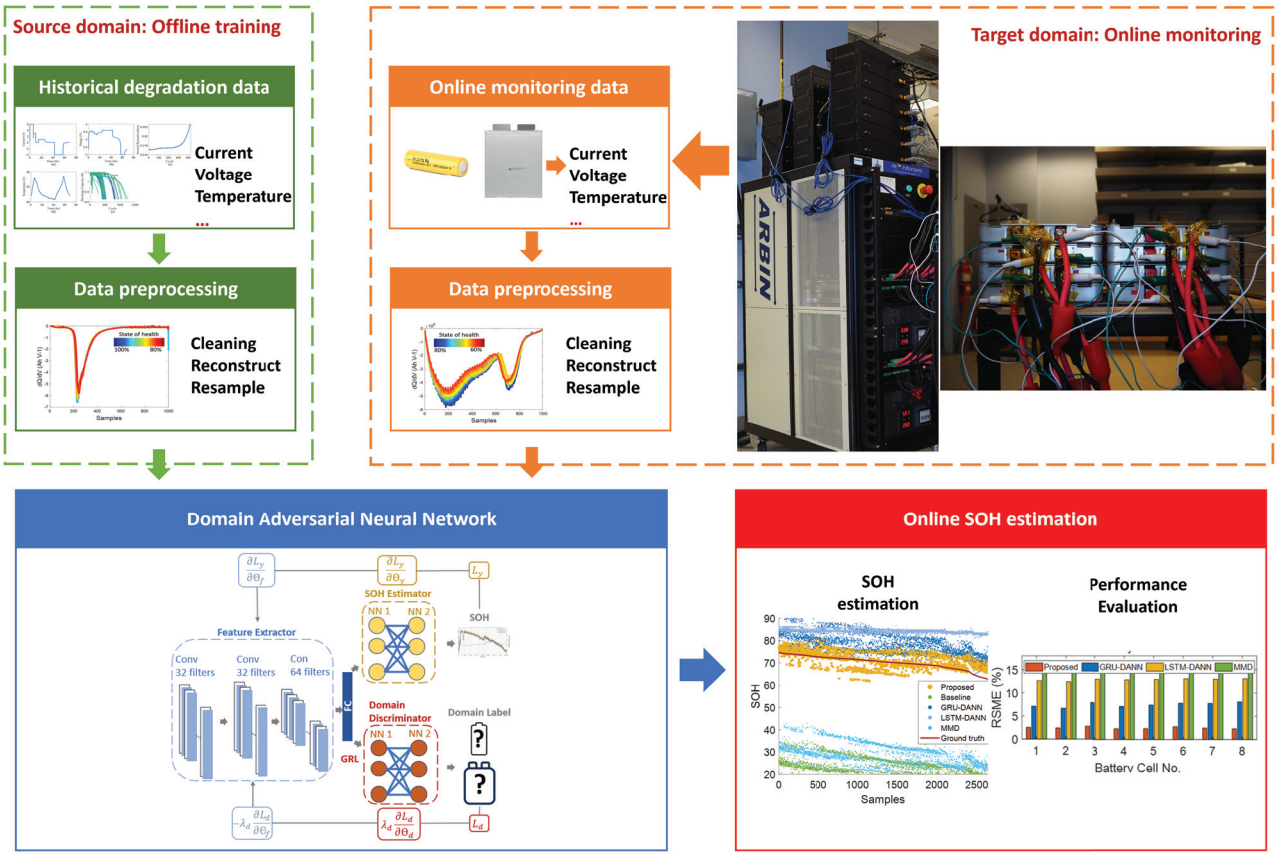

Fig. 1. Flow diagram for the proposed methodology.

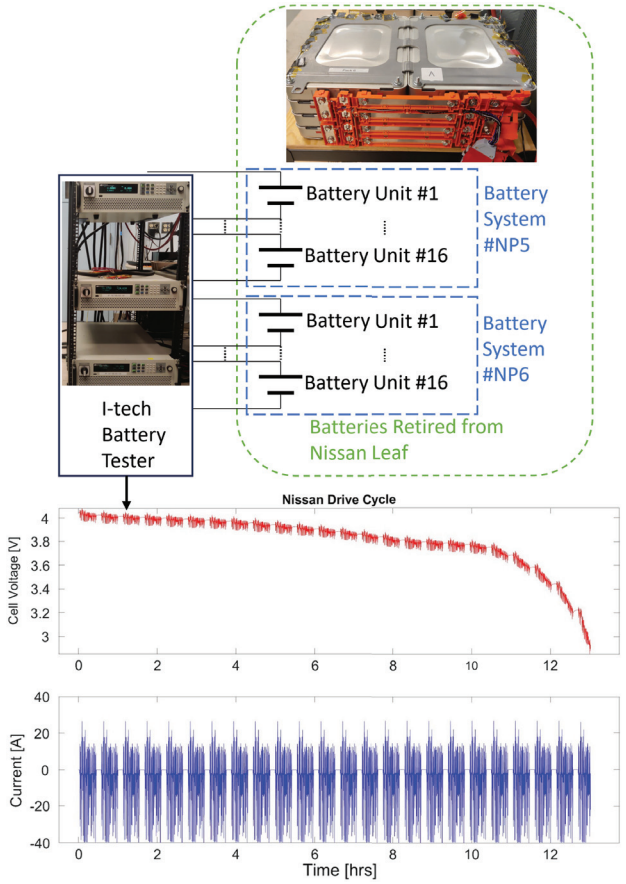

Fig. 2. Experimental setup for second-life battery testing using Nissan Leaf retired batteries.

the same discharge policy but various fast-charging policies. The dataset presented a complete aging trajectory at varying usage conditions, accompanied by operation features like charging capacity, discharging capacity, current, voltage, internal resistance, and temperature. The overall number of testing cycles ranges from 150 to 2,300, compiled into three batches, with each representing approximately 48 cells. The temperature measurements were performed by attaching a Type T thermocouple with thermal epoxy and Kapton tape to the exposed cell can after stripping a small section of the plastic insulation. Internal resistance measurements were obtained during charging at 80% SOC by averaging 10 pulses of 3.6C with a pulse width of 30–33 ms. Details on both datasets are provided in Table I.

B. DATA PREPROCESSING

The data preprocessing step is crucial for preparing the dataset for effective model training and subsequent analysis. The process consists of organizing data, cleaning noise, and removing inconsistent samples. Additionally, unlike conventional data processing, which often involves feature extraction, our approach involves constructing a derivative curve directly from the raw measurements.

The raw data, comprising current, voltage, internal resistant, and temperature measurements from the battery cells are first organized for each cycle of each battery cell. This organization aids in the subsequent steps of noise cleaning and curve generation, ensuring consistency across the dataset. Noise in the data, which can arise from measurement inaccuracies or external disturbances, is mitigated through a combination of filtering techniques. Data points that deviate significantly from expected behavior are identified and removed. This includes outlier detection where measurements are inconsistent with the rest of the dataset, possibly due to sensor errors or faulty cell operations. Outliers are detected using statistical thresholds.

Instead of traditional feature extraction, our preprocessing involves generating a differential capacity curve (dQ/dV) directly from the cleaned current (I) and voltage (V) data. The dQ/dV curve, which represents the derivative of capacity with respect to voltage, is calculated by numerically differentiating the charge capacity (Q) with respect to voltage. This curve is pivotal as it highlights the characteristic peaks correlating to specific electrochemical processes within the battery cell, serving as a direct input feature for our neural network model.

Finally, to ensure uniformity across different datasets, all generated dQ/dV curves are normalized to the same scale using a unified Min-Max scaling approach. This technique involves identifying the global minimum and maximum values across all datasets prior to normalization. The normalization is conducted using the formula:

$$X_{\text{norm}} = \frac{X - X_{\text{global min}}}{X_{\text{global max}} - X_{\text{global min}}} \tag{1}$$

where X is the original value, $X_{\text{global min}}$ is the minimum value found across all datasets, and $X_{\text{global max}}$ is the maximum value across all datasets. By applying the same scale to all datasets, the neural network is better equipped to handle variations in data from different sources without bias or scale-related distortions.

C. FEATURE EXTRACTION BASED ON CNN NETWORK

CNNs have become one of the most popular deep learning models in the analysis of data that contains spatial or temporal patterns, such as images or time-series data. This makes them particularly well suited for processing the dQ/dV curves derived from battery charge–discharge cycles, which are rich in temporal patterns and characteristics indicative of battery health.

Table I. Main specifications of the selected LIBs

Dataset	Manufacturer/ Provider	Electrode Active Materials (Cathode/Anode)	Nominal Capacity (ah)	Voltage Range (V)	Data Amount (Samples)	SOH Range	Operation Condition
#1	A123/MIT public	LFP/graphite	1.1 Ah	2–3.6V	124	80–100%	4C Fast-charging
#2	Nissan Leaf/ private	$LiMn_2O_4$ with $LiNiO_2$/graphite	33.1 Ah	2.6–4.2V	9	60–80%	Day-Ahead and Real-Time Energy Timing Shift (DART)

A typical CNN architecture comprises convolutional layers, activation functions, pooling layers, and fully connected layers. Convolution layers are the core building blocks of a CNN. They apply a set of learnable filters to the input. Each filter captures specific features from the data at various spatial or temporal resolutions. Activation functions refer to nonlinear activation functions, such as the rectified linear unit (ReLU), are applied to the output of the convolutional layers. This step introduces nonlinearity into the model, enabling it to learn complex features. Pooling layers reduce the spatial or temporal size of the feature maps, thereby decreasing the number of parameters and computation in the network. Pooling can be performed in various ways, such as max pooling or average pooling.

Using CNNs allows for a robust analysis of battery data with several advantages. CNNs are capable of automatically detecting important features without the need for manual intervention. This is crucial in battery data analysis where key features may not be immediately apparent or are difficult to extract manually. CNNs also learn hierarchies of features. Lower layers might detect simple edges or transitions in dQ/dV curves, while deeper layers can identify complex patterns that are more abstract and represent the underlying electrochemical processes. During training, CNNs can be easily adapted and retrained to handle data from different battery types or operating conditions, enhancing the versatility of the battery health monitoring system. Once trained, CNNs can process new data rapidly, making them suitable for energy storage applications where real-time analysis is critical.

D. PROPOSED CNN-DANN MODEL FOR SOH ESTIMATION

A DANN is designed to predict SOH in batteries, referred to as one-dimensional CNN-DANN, as shown in Fig. 3. It consists of two stages specifically designed to the SOH prediction problem. The convolutional layers in CNNs are adept at identifying temporal patterns and anomalies within the sequential data, encoding them into representations. This capability makes CNNs ideal for analyzing dQ/dV curves, where subtle changes in the curve can be extracted as important health indicators of the battery. Additionally, CNNs can recognize both local and global patterns in the dQ/dV curves. By applying different filters and kernel sizes, CNNs can capture a wide range of dependencies and features across the curve, from short-term changes to long-term trends, which are indicative of various degradation mechanisms. A model trained in one domain may perform poorly in another domain. The use of DANNs in our methodology addresses the challenge of domain discrepancy. By aligning the representations from different domains, DANNs help in learning features that are not only relevant to the health estimation task but also invariant across different operational domains, thereby improving the model's generalizability and robustness. This approach of using CNNs and DANNs for one-dimensional dQ/dV curve data combines the deep learning strengths in pattern recognition with capabilities in domain adaptation.

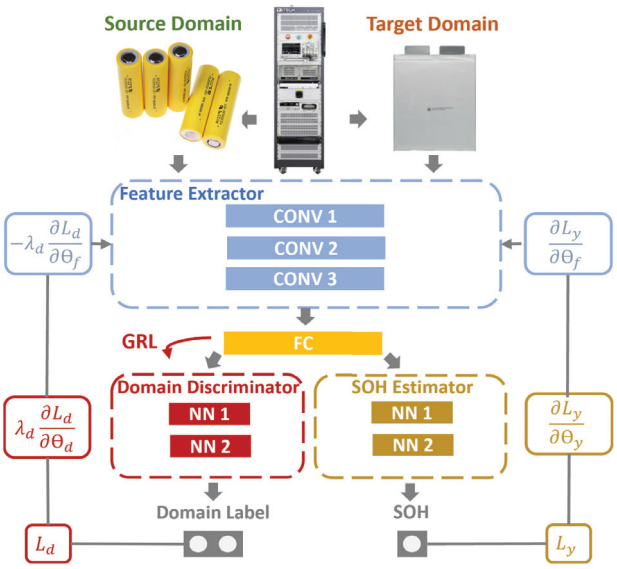

Fig. 3. Illustrative overview of the proposed DANN.

Stage 1: It contains a 1D CNN model to extract features from the battery data. These features may include temporal patterns in voltage, current, temperature, and other related battery signals. The feature extraction process at this stage can be expressed as:

$$y_i^{(l)} = f\left(\sum_{j=0}^{k-1} W_{ij}^{(l)} \cdot x_{i+j}^{(l-1)} + b_i^{(l)}\right) \tag{2}$$

$$d_i^{(l)} = y_i^{(l)} \cdot r_i^{(l)} \tag{3}$$

$$z_i^{(l)} = \max\left(y_{i\cdot s}^{(l)}, y_{i\cdot s+1}^{(l)}, \ldots, y_{i\cdot s+s-1}^{(l)}\right) \tag{4}$$

where the convolution operation is applied to the input signal, using a set of kernels. $y_i^{(l)}$ is the output of the i-th neuron in layer l. $x_{i+j}^{(l-1)}$ is the input to the convolution layer from the previous layer or the original input signal. $W_{ij}^{(l)}$ represents the weight between the i-th neuron and the j-th element in the kernel at layer l. $b_i^{(l)}$ is the bias term for the i-th neuron at layer l. k is the size of the convolutional kernel. f is the activation function, often a ReLU or another nonlinear function. During training, a certain fraction of the neurons is randomly set to zero, effectively "dropping out" those neurons from the network for that specific iteration. $d_i^{(l)}$ is the output of the i-th neuron after applying dropout at layer. $y_i^{(l)}$ is the input to the dropout layer (output of the previous layer). $r_i^{(l)}$ is a random variable that takes the value of 0 with probability p (the dropout rate) and 1 otherwise. Pooling layers are then used to reduce the dimensionality of the data, which can help the model focus on the most essential features. $z_i^{(l)}$ is the output of the i-th neuron in the pooling layer. $y_i^{(l)}$ is the input to the pooling layer from the previous convolution layer. s is the stride or size of the pooling operation.

Stage 2: This stage leverages the extracted features and focuses on addressing the domain shift problem. It consists of two neural network parts: the label predictor and the domain classifier. The former targets accurate SOH prediction, while the latter aims to erase the differences between source and target domains. By training these parts simultaneously in an adversarial manner, DANN ensures that the model's predictive ability is complemented by its adaptability to different domains. The DANN equation can be expressed as:

$$y_{L+1} = \phi(\alpha_{L+1} y_L + \beta_{L+1}) \tag{5}$$

$$p_{ij} = y_{L+M+Z+1} \tag{6}$$

$$d_k = \psi(\Upsilon_k y_k + \delta_k), \qquad k \in \{1,2,\ldots,D\} \tag{7}$$

$$L = L_{\text{SOH}} - \lambda L_{\text{domain}} \tag{8}$$

where the first equation focuses on predicting the actual output labels without considering the domain differences between the source and target datasets. It takes the features extracted by the 1D CNN and attempts to map them to the SOH values. $\psi(x)$ from the second equation denotes the activation function in domain classification, and d_k is the output related to domain discrimination. The combined training of the 1D CNN, label predictor, and domain classifier requires a joint loss function that balances the objectives of accurate SOH prediction and effective domain adaptation, where L_soh is the loss for SOH prediction, L_domain is the loss for domain classification, and λ is a hyperparameter controlling the balance between the two.

The proposed 1D CNN-DANN model for battery SOH estimation combines the strength of CNNs in feature extraction with the adaptability of domain adversarial training. The formal steps of this methodology are detailed in Algorithm 1, and this two-stage approach promises a versatile and robust model capable of operating seamlessly across different battery chemistries, SOH ranges, and operational conditions.

E. COMPARATIVE METHODS

In this section, the performance of the proposed CNN-DANN method on battery SOH estimation is compared with three other transfer learning including gated recurrent unit (GRU)-DANN, LSTM-DANN, and maximum mean discrepancy (MMD). GRU-DANN is selected for comparison due to its architectural efficiency and capability to process time-series data effectively. GRUs are known for their simpler structure compared to LSTMs, which often allows for faster training times without sacrifice in performance. This makes GRU-DANN a valuable baseline for scenarios where computational resources or data availability are constrained. LSTM-DANN is included due to its proficiency in capturing long-term dependencies in sequence data, a common feature in battery usage cycles. LSTMs are capable of overcoming vanishing gradient problems better than traditional recurrent neural networks, making them highly suitable for modeling complex patterns over extended periods. This comparison aims to assess whether the additional complexity of LSTMs translates into better SOH estimation accuracy when coupled with domain adaptation. MMD is a powerful nonparametric measure used in domain adaptation to quantify the difference between the source and target domain distributions. Comparing MMD with DANN-based methods provides insight into how well domain discrepancy can be mitigated purely through statistical means, offering a contrast to the deep learning-based approaches.

The comparison among these methods allows the examination of how different architectures and adaptation mechanisms can influence the robustness and accuracy of SOH estimations under varying operational conditions and

Algorithm 1: CNN-DANN for SOH Estimation.

Input: Source domain dataset D_s, target domain dataset D_t, learning rates η_f, η_d, η_c., number of epochs E

Output: Trained CNN-DANN model capable of SOH estimation on target domain

1. **Initialize Parameters:** Initialize the parameters of the feature extractor layers F, the domain classifier layers D, and the label predictor layers C.
2. **For each epoch e from *1* to *E*:**
   a. For each batch b in D_s and D_t:
      Extract Features:
      I. X_s, y_s = next batch from D_s
      II. X_t = next batch from D_t
      III. Use F to extract features $f_s = F(X_s)$ and $f_t = F(X_t)$
   b. Domain Classification
      I. Concatenate f_s and f_t to form f_c
      II. Predict domain labels $d = D(f_c)$ using domain classifier D
      III. Calculate domain classification loss L_D using the true domain labels and d
   c. Label Prediction (only for source domain)
      I. Predict labels $y_S = C(f_S)$ using label predictor C
      II. Calculate label prediction loss L_C using the true labels y_S
   d. Backpropagation and Parameter Update:
      I. Calculate total loss $L = L_c - \lambda L_D$ where λ is the trade-off weight
      II. Update F using gradient descent with learning rate η_f
      III. Update D using gradient descent with learning rate η_d
      IV. Update C using gradient descent with learning rate ηc
3. **End For**
4. **Return**: Return the trained model components F, C, D.

dataset characteristics. By comparing the performance of these models, this study aims to highlight the specific advantages of using CNN-DANN for battery estimation and to identify potential areas where alternative models may offer preferable outcomes.

F. EVALUATION METRICS

The testing set was used to evaluate the transfer learning model's ability to estimate the SOH. Performance metrics such as root mean squared error (RMSE) and mean absolute error (MAE) were calculated to quantify the model's accuracy and reliability. Specifically, we calculated the errors mentioned above with formulas as follows:

$$\mathrm{RMSE} = \sqrt{\frac{1}{N}\sum_{N=1}^{N}(y_i - \hat{y}_i)^2} \tag{9}$$

$$\mathrm{MAE} = \frac{1}{N}\sum_{N=1}^{N}|y_i - \hat{y}_i| \tag{10}$$

In these equations, y_i represents ground-truth label, $\hat{y}_i$ represents the model's prediction, and N is the total number of samples.

III. RESULTS AND DISCUSSION

A. ANALYSIS OF dQ/dV CURVES AS INPUT FEATURES

The dQ/dV curve, illustrated in Fig. 4, represents the differential capacity (dQ) as a function of the potential voltage difference (dV) and is known to be highly sensitive to changes in the internal structure and condition of the battery [14]. The left graph presents data from an MIT A123 battery (#b1c0), while the right graph features a Private Nissan Leaf battery (#NP5). These curves are input features for the transfer learning models, helping to estimate the SOH across different battery chemistries and operational conditions.

The dQ/dV curves show distinct peak patterns and baseline shifts, indicating the influence of different battery chemistries, operational histories, and SOH ranges. The MIT A123 battery demonstrates a single peak, which shifts upward as the battery degrades from 100% to 80% SOH. In contrast, the Nissan Leaf battery displays multiple peaks, with the entire set of peaks shifting upward as the SOH decreases from 80% to 60%. Despite the differences in peak number and shape, a consistent trend is observed across both types of batteries. As the battery ages, regardless of the type, SOH range, or operational conditions, the entire dQ/dV curve shifts upward. This upward movement is a key indicator of degradation, as it reflects the increased resistance and decreased efficiency of the battery at higher cycle numbers. The uniform degradation pattern captured by the dQ/dV curves is crucial for the CNN-DANN model's ability to learn from one domain and effectively transfer that knowledge to another.

B. TRANSFER EXPERIMENTS

The designed transfer experiments as shown in Fig. 5 explore the effectiveness of the proposed CNN-DANN approach in transferring knowledge from a well-characterized source domain to a less-characterized target domain. The experiments are structured to simulate a realistic scenario where sufficient cycling data is available for battery cells from source domain, but very limited data is available for the target domain. For the purpose of these experiments, we arbitrarily selected 1000 cycles data from 124 cells of the source domain. In contrast, the target domain is significantly more restricted, consisting of data

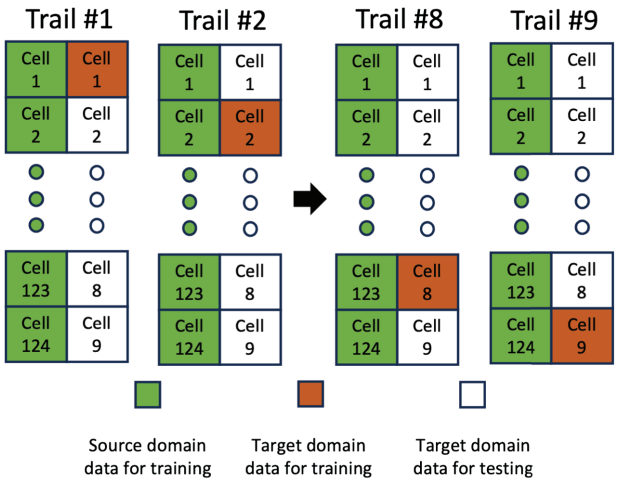

Fig. 5. The experiment design of 9 trail runs for transfer learning.

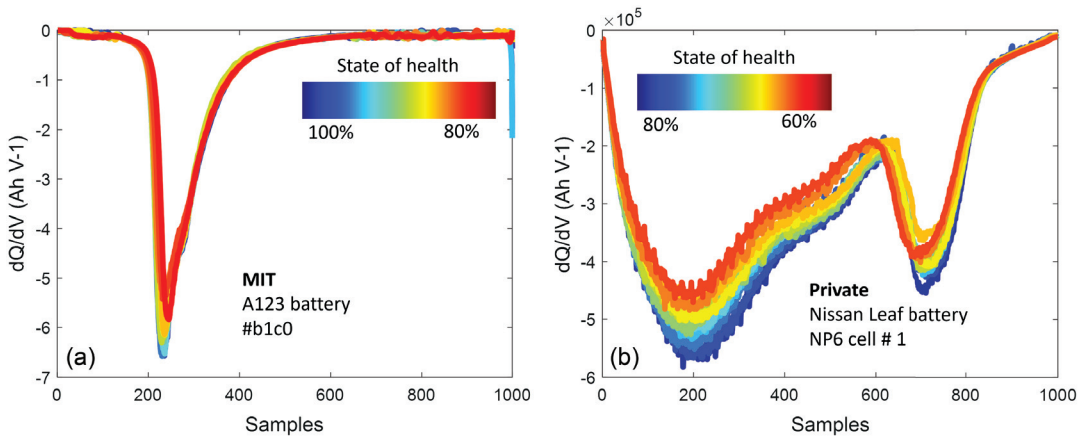

Fig. 4. Voltage–capacity discharge curves. a, dQ/dV from A123 battery. b, dQ/dV from Nissan Leaf battery.

from only 9 cells. Initially, we select one cell's data as unlabeled data from the target domain for training the model, simulating a real-world scenario where sufficient labeled data is unavailable. The remaining eight cells are used as testing data to evaluate the model's ability to generalize and accurately estimate battery SOH based solely on the transferred knowledge and the minimal unlabeled data from the target domain.

Despite the promising applications of deep learning in SOH estimation, the reliability of deep learning methods remains under investigation due to their complex, often refer as black boxes. Ongoing research, such as demonstrated in [44], continues to explore and address these reliability issues, emphasizing a solution for utilizing a framework that derives SOH results from the quantile distribution of deep features, providing associated confidence interval. Additionally, it employs a novel Wasserstein distance-based quantile Huber (QH) loss function that integrates Huber loss with quantile regression loss for optimized model training based on distribution outputs. To address concerns regarding the transparency and reliability of deep learning models, we have conducted the experiment across nine trails, where different subsets of source and target data are utilized to train and test the model, as illustrated in Fig. 5. Each trail helps in assessing the stability and consistency of the model across varying conditions within the target domain. The arbitrary selection of samples for each trail ensures a robust evaluation under diverse conditions, aiding in mitigating the "black box" nature by providing reproducible evidence of the model's performance.

C. IMPLEMENTATION DETAILS

The dQ/dV curves were first processed to ensure uniformity in input data structure, being sampled to 1000 data points per curve. This standardization is for maintain consistency in feature extraction across different battery cells. The sampled data points were then used as input for the one-dimensional CNN-DANN network.

The structure of the CNN-DANN used in this study is detailed in Table II. Key hyperparameters of the model include CNN layers, filter size, batch size, learning rate, dropout rate, and epochs. The network features three sets of layers with 32, 32, and 64 filters, respectively, allowing for a progressive feature extraction from raw input data. Each filter has a size of 3, which is typical for capturing local dependencies within the sequence data. Batch size is set at 87, optimizing the balance between training speed and memory usage. A rate of 0.0001 is used as the learning rate to ensure stable convergence during training. The dropout rate is set at 0.5 to provide regularization to prevent overfitting. The network is trained for 250 epochs, allowing sufficient time for the model to learn the patterns inherent in the battery data.

Table II. Proposed model parameters

Parameter	Meaning	Value
J	Number of CNN layers	[32, 32, 64]
P	Filter size	3
l	Batch size	87
L	Learning rate	0.0001
M	Dropout	0.5
E	Epochs	250

The feature extraction part of the model is first trained using the source domain data. After feature extraction, the output from the CNN feeds into a fully connected layer designed to estimate the SOH of the battery. This layer functions as the SOH estimator and consists of two layers which process the features to produce a prediction of the battery's health. Simultaneously, the DANN is employed to address the challenge of domain adaptation. This part includes a label classifier, which also comprises two fully connected layers. The label classifier's task is to predict the domain of each input sample, trying to distinguish between the source and target domains. The training involves a unique adversarial process where the model learns to minimize the ability of the label classifier to determine the domain of the data while still maintaining its ability to accurately predict the SOH. This adversarial training helps in making the feature extractor domain-invariant, enhancing the model's ability to generalize from the source to the target domain without loss in performance.

By incorporating these layers, the CNN-DANN model not only learns the specific features related to SOH but also adapts to handle data from different domains, thus addressing the key challenge in applying machine learning models to real-world scenarios where data conditions can vary significantly.

D. VISUALIZATION OF FEATURE DISTRIBUTIONS

In deep learning frameworks, especially when dealing with complex input such as the dQ/dV curves from battery systems, it is important to measure the significance and applicability of autonomously extracted features. Unlike conventional machine learning approaches where feature engineering is manually achieved, the CNNs within our model autonomously extract features from raw data. This automated feature extraction needs an investigation into whether the derived features are robust and discriminative for tasks such as domain adaptation and SOH estimation in batteries. To address this, we employ dimensionality reduction techniques to visualize and compare the feature distributions as learned by the model.

To visualize the feature distribution, we utilize t-distributed stochastic neighbor embedding (t-SNE), a machine learning algorithm designed for the visualization of high-dimensional data by embedding it into a two-dimensional space. This method is particularly chosen for its proficiency in maintaining the local structure of the data, thereby allowing us to visually assess the clustering tendency and separation between features from low-dimensional domains. Through t-SNE, we can observe whether the features encapsulate distinct characteristics of the data indicative of different operational domains and degradation states.

The t-SNE visualizations in Fig. 6. illustrate the spatial distribution of features corresponding to the source and target domains for models trained using different architectures, including CNN-DANN, GRU-DANN, LSTM-DANN, and MMD. Ideal feature representation should exhibit substantial overlap between domains, indicating effective domain adaptation. The CNN-DANN model demonstrates a higher degree of feature overlap between domains, suggesting superior capability in feature

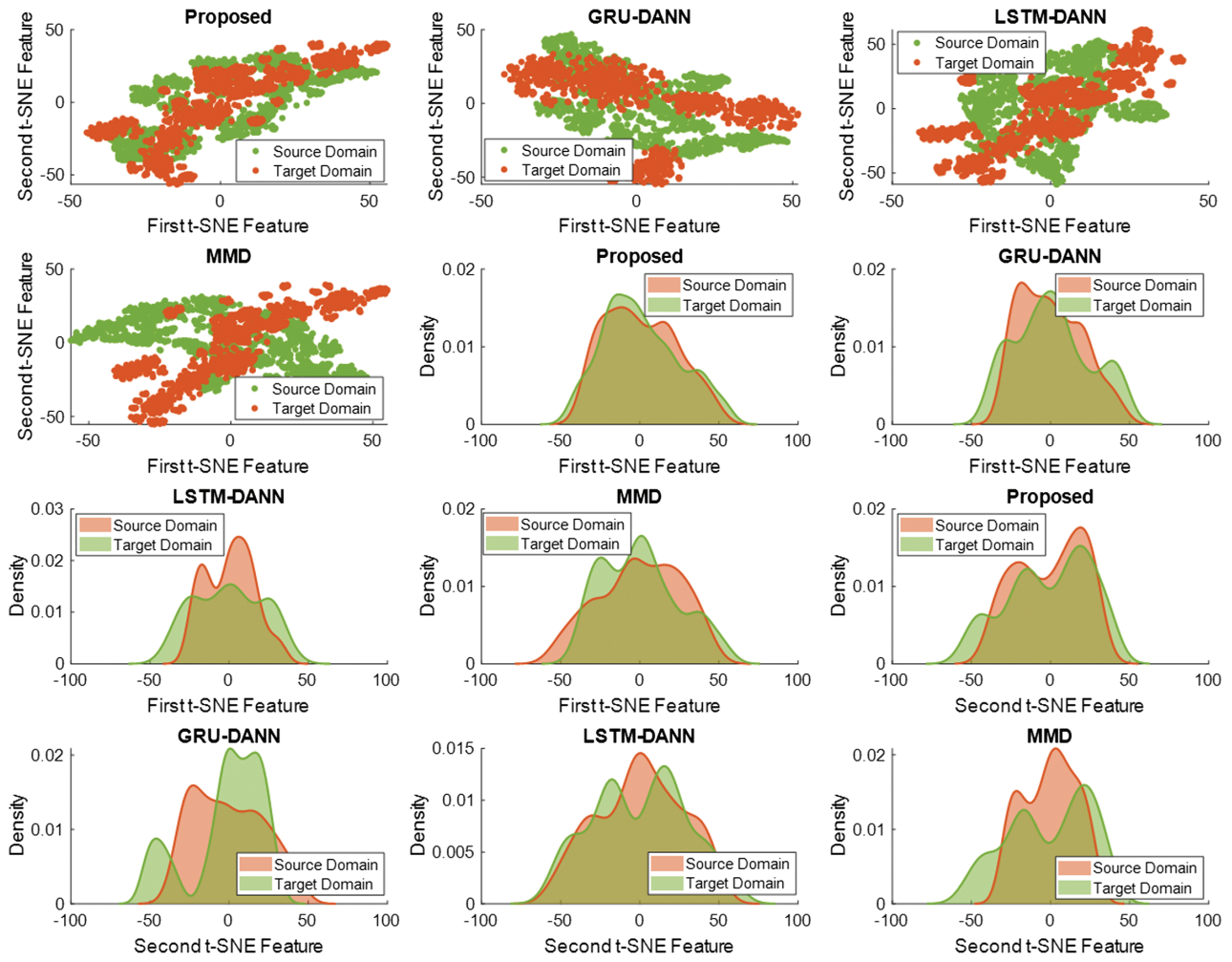

Fig. 6. t-SNE visualization of A123 batteries and Nissan batteries.

extraction across diverse battery chemistry, SOH range, and operational conditions.

Further down, the density plots of the first and second t-SNE features in Fig. 6. offer a quantitative perspective on the density distribution of the features across domains. The CNN-DANN model not only shows greater overlap in the first-SNE feature but also maintains consistency across the second feature, indicating robust generalization capabilities across domains. In contrast, the divergence observed in the plots for other models signifies less effective adaptation.

E. COMPARISONS WITH OTHER DATA-DRIVEN METHODS

In this section, the performance of the proposed method on battery SOH estimation is compared with three other transfer learning methods, including GRU-DANN, LSTM-DANN, and MMD. Table III presents the estimation performance of methods using the average values from 10 trails. The proposed CNN-DANN method showcases superior estimation performance, in terms of RMSE and MAE.

Table III. Overall comparisons with all data-driven methods

	Proposed		GRU-DANN		LSTM-DANN		MMD	
Testing Battery Cells	**MAE**	**RSME**	**MAE**	**RSME**	**MAE**	**RSME**	**MAE**	**RSME**
#1	1.97	2.56	6.86	7.11	12.53	12.66	14.51	14.69
#2	1.60	2.42	6.41	6.68	12.30	12.44	14.81	14.99
#3	2.26	2.79	7.71	7.92	12.86	12.98	14.21	14.40
#4	1.24	2.34	6.92	7.14	12.71	12.85	15.13	15.26
#5	1.26	2.35	7.19	7.44	12.78	12.92	15.00	15.13
#6	2.11	2.78	7.46	7.81	12.94	13.07	13.97	14.25
#7	1.75	2.48	7.56	7.80	12.85	12.99	14.28	14.47
#8	1.25	2.30	7.94	8.12	12.95	13.09	14.84	14.97

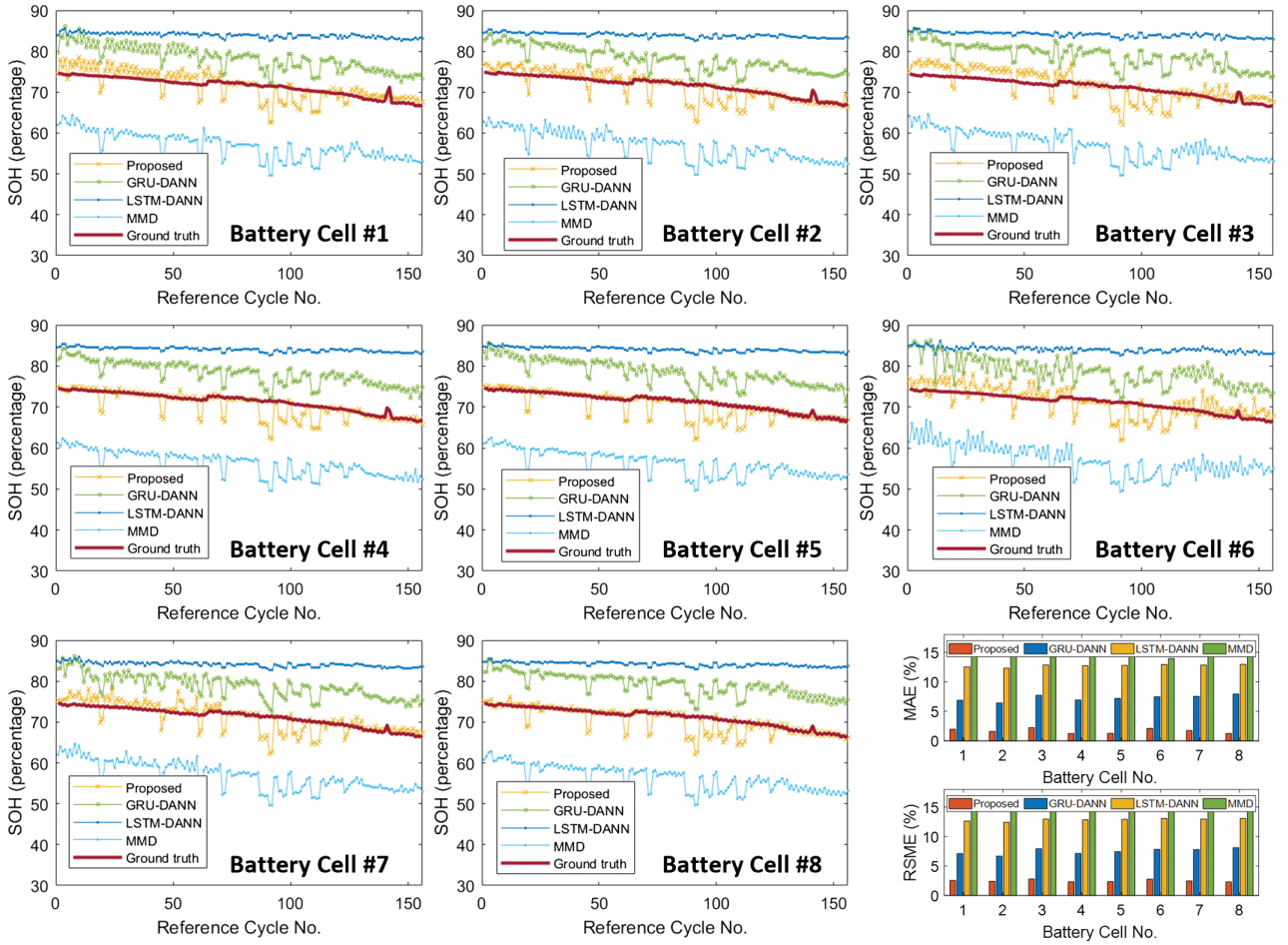

Fig. 7. SOH estimation performance analysis using various methods.

Figure 7 illustrates the estimation results for 8 cells from target domain. The MMD method exhibited the highest MAE and RMSE value among the four approaches, reflecting its limitation as a statistical approach that may not align well with the practical complexities of battery degradation. The LSTM-DANN kept the MAE and RMSE below 12.74% and 12.88%. It exhibits moderately higher error rates; this could be caused by struggling with capturing the full complexity of degradation patterns without extensive tuning or larger datasets. GRU-DANN shows reasonable tracking of the SOH trend. The GRU-DANN kept the MAE and RMSE below 7.26% and 7.5%, suggesting less effective adaptation on feature extraction in comparison to the MAE and RMSE of 1.68% and 2.50% from CNN-DANN.

The bar graphs illustrate the comparative analysis of MAE and RMSE for each battery cell from target test data, highlighting the consistent superiority of the proposed CNN-DANN model over the other methods. This improvement reveals the proposed model's estimation accuracy, adaptability to varying SOH condition, and robustness against variations in battery chemistry and operational scenarios. This performance is crucial for applications like battery health monitoring, where accurate and reliable predictions are essential for operational safety and efficiency.

To further investigate the robustness of our proposed method under conditions of limited data availability, we conducted additional experiments where only partial segments (80% and 60%) of the dQ/dV curve were utilized. This approach simulated more challenging scenarios frequently encountered in practical applications where complete data may not be accessible. Our findings indicate a progressive increase in prediction error as the amount of available data decreases: utilizing 80% of the dQ/dV curve resulted in the MAE and RMSE of 2.12% and 3.43%, while reducing the data to 60% led to a higher MAE and RMSE of 4.42% and 6.76%. These results underscore the importance of data completeness in achieving accurate SOH estimation and highlight the capability of our model to provide reliable predictions even with reduced data.

IV. CONCLUSION

This paper presents a domain adaptation model for second-life battery SOH estimation, utilizing one-dimensional CNN and DANN. The proposed approach is designed to be lightweight, allowing for efficient adaptation and prediction with minimal unlabeled data requirements from the target domain. We demonstrate that even with the data of only one unlabeled target battery cell, our method is capable of transferring the knowledge from the source batteries. This has significant practical implications:

Data Economy: The ability to make accurate predictions with minimal target domain data is essential in scenarios where collecting large quantities of labeled data is challenging, time-consuming, or costly.

Scalability: The method can be readily applied to any new or used battery types or operating conditions without the need for extensive retraining or additional data collection.

Resource Efficiency: The lightweight design means lower computational requirements, making the algorithm suitable for real-time applications or resource-constrained environments.

Our future work plans are to investigate various battery chemistries. By doing so, we aim to test the generalization and robustness of our model. Lastly, implementing and testing the model in actual industrial settings for second-life energy storage applications will be essential for evaluating its practicality, efficiency, and effectiveness in real-world conditions.

CONFLICT OF INTEREST STATEMENT

The authors declare no conflicts of interest.

REFERENCES

[1] M. Shahjalal, P. Roy, T. Shams, A. Fly, J. Chowdhury, M. Ahmed, and K. Liu "A review on second-life of Li-ion batteries: prospects, challenges, and issues," *Energy*, vol. 241, p. 122881, 2022.

[2] C. Font, H. Siqueira, J. Neto, J. Santos, S. Stevan, A. Converti, and F. Correa "Second life of lithium-ion batteries of electric vehicles: a short review and perspectives," *Energies*, vol. 16, p. 953, 2023.

[3] T. Montes, M. Etxandi-Santolaya, J. Eichman, V. Ferreira, L. Trilla, and C. Corchero "Procedure for assessing the suitability of battery second life applications after EV first life," *Batteries*, vol. 8, p. 122, 2023.

[4] J. Zhu, I. Mathews, D. Ren, W. Li, D. Cogswell, B. Xing, T. Sedlatschek, S. Kantareddy, M. Yi, T. Gao, Y. Xia, Q. Zhou, T. Wierzbicki, and M. Bazant "End-of-life or second-life options for retired electric vehicle batteries," *Cell Rep. Physical Sci.*, vol. 2, p. 100537, 2021.

[5] P. Chombo and Y. Laoonual "A review of safety strategies of a Li-ion battery," *J. Power Sources*, vol. 478, p. 228649, 2020.

[6] S. Pradhan and B. Chakraborty "Battery management strategies: an essential review for battery state of health monitoring techniques," *J. Storage Mater.*, vol. 51, p. 104427, 2022.

[7] X. Zhao, Z. Wang, E. Li, and H. Miao "Investigation into impedance measurements for rapid capacity estimation of lithium-ion batteries in electric vehicles," *J. Dynamic, Monitoring Diagnostics*, vol. 3, pp. 21–31, 2024.

[8] P. Makeen, H. Ghali, S. Memon, and F. Duan "Electric vehicles lithium-polymer ion battery dynamic behaviour charging identification and modelling scheme," *J. Dynamic, Monitoring Diagnostics*, vol. 2, pp. 170–176, 2023.

[9] J. Bokstaller, J. Schneider, and J. Brocke "Estimating SoC, SoH, or RuL of rechargeable batteries via IoT: a review," *IEEE Internet Things*, vol. 99, pp. 1–1, 2023.

[10] L. Yao, S. Xu, A. Tang, F. Zhou, J. Hou, Y. Xiao, and Z. Fu "A review on state of health estimations and remaining useful life prognostics of lithium-ion batteries," *World Electr. Veh. J.*, vol. 2, p. 113, 2021.

[11] Y. Preger, H. Barkholtz, A. Fresquez, D. Campbell, B. Juba, J. Kustas-Roman, S. Ferreira, and B. Chalamala "Degradation of commercial litthium-ion cells as a function of chemistry and cycling conditions," *J. Electrochem. Soc.*, vol. 167, p. 120532, 2020.

[12] J. Pender, G. Jha, D. Youn, J. Ziegler, I. Andoni, E. Choi, A. Heller, B. Dunn, P. Weiss, R. Penner, and C. Mullins "Electrode degradation in lithium-ion batteries," *ACS Nano*, vol. 14, pp. 1243–1295, 2020.

[13] J. Zhao, X. Han, M. Ouyang, and A. Burke "Specialized deep neural networks for battery health prognostics: opportunities and challenges," *J. Energy Chem.*, vol. 87, pp. 416–438, 2023.

[14] J. Lu, R. Xiong, J. Tian, C. Wang, and F. Sun "Deep learning to estimate lithium-ion battery state of health without additional degradation experiments," *Nat. Commun.*, vol. 14, p. 2760, 2023.

[15] F. Wang, Z. Zhai, Z. Zhao, Y. Di, and X. Chen "Physics-informed neural network for lithium-ion battery degradation stable modeling and prognosis," *Nat. Commun.*, vol. 15, p. 4332, 2024.

[16] D. Roman, S. Saxena, V. Robu, M. Pecht, and D. Flynn "Machine learning pipeline for battery state-of-health estimation," *Nat. Mach. Intell.*, vol. 3, pp. 447–456, 2021.

[17] N. Yang, Z. Song, H. Hofmann, and J. Sun "Robust State of Health estimation of lithium-ion batteries using convolutional neural network and random forest," *J. Storage Mater.*, vol. 48, p. 103857, 2022.

[18] A. Naha, S. Han, S. Agarwal, A. Guha, A. Khandelwal, P. Tagade, K. Hariharan, S. Kolake, J. Yoon, and B. Oh "an incremental voltage difference based technique for online state of health estimation of Li-ion batteries," *Sci. Rep.*, vol. 10, p. 9526, 2020.

[19] M. Zhang, D. Yang, J. Du, H. Sun, L. Li, L. Wang, and K. Wang "A review of SOH prediction of Li-ion batteries based on data-driven algorithms," *Energies*, vol. 16, p. 3167, 2023.

[20] T. Feng, L. Yang, X. Zhao, H. Zhang, and J. Qiang "Online identification of lithium-ion battery parameters based on an improved equivalent-circuit model and its implementation on battery state-of-power prediction," *J. Power Sources*, vol. 281, pp. 192–120, 2015.

[21] M. Streb, M. Andersson, V. Klass, M. Klett, M. Johansson, and G. Lindbergh "Investigating re-parametrization of electrochemical model-based battery management using real-world driving data," *eTransportation*, vol. 16, p. 100231, 2023.

[22] Y. Zhang and Y. Li "Prognostics and health management of lithium-ion battery using deep learning methods: a review," *Renewable Sustainable Energy Rev.*, vol. 161, p. 112282, 2022.

[23] X. Chen, X. Li, S. Yu, Y. Lei, N. Li, and B. Yang "Dynamic vision enabled contactless cross-domain machine fault diagnosis with neuromorphic computing," *IEEE/CAA J. Autom. Sin.*, vol. 11, pp. 788–790, 2024.

[24] H. Yang, X. Wang, S. Zheng, M. Xu, and X. Li "Prediction of solid rocket motor performance based on deep learning and ignition experimental data," In IEEE Transactions on Aerospace and Electronic Systems, 2024.

[25] E. Vanem, Q. Liang, M. Bruch, G. Bothun, K. Bruvik, K. Thorbjornsen, and A. Bakdi "Statistical models for condition monitoring and state of health estimation of lithium-ion batteries for ships," *J. Dynamic, Monitoring Diagnostics*, vol. 3, pp. 11–20, 2024.

[26] J. Reniers, G. Mulder, and D. Howey "Review and performance comparison of mechanical-chemical degradation models for lithium-ion batteries," *J. Electrochem. Soc.*, vol. 166, pp. A3189–A3200, 2019.

[27] V. Sulzer, P. Mohtat, A. Aitio, S. Lee, Y. Yeh, F. Steinbacher, M. Khan, J. Lee, J. Siegel, A. Stefanopoulou, and D. Howey

"The challenge and opportunity of battery lifetime prediction from field data," *Joule*, vol. 5, pp. 1934–1955, 2019.

[28] M. Chen, G. Ma, W. Liu, N. Zeng, and X. Luo "An overview of data-driven battery health estimation technology for battery management system," *Neurocomputing*, vol. 531, pp. 152–169, 2023.

[29] Y. Zhang, Y. Li, M. Zhang, and H. Wang "A novel health indicator by dominant invariant subspace on graassmann manifold for state of health assessment of lithium-ion battery," *Eng. Appl. Artif. Intell.*, vol. 130, p. 107698, 2024.

[30] X. Li, W. Zhang, X. Li, and H. Hao "Partial domain adaptation in remaining useful life prediction with incomplete target data," *IEEE/ASME Trans. Mechatron.*, vol. 29, pp. 1903–1913, 2023.

[31] B. Yang, Y. Lei, Y. Li, N. Li, and A. Nandi. "Label recovery and trajectory designable network for transfer fault diagnosis of machines with incorrect annotation," *IEEE/CAA J. Autom. Sin.*, vol. 11, pp. 932–945, 2024.

[32] J. Jiang "A literature survey on domain adaptation of statistical classifiers," 2008, http.sifaka.cs.uiuc.edu/jiang4/domainadaptation/survey.

[33] S. Siahpour, X. Li, and J. Lee "Data-driven prediction of battery cycle life before capacity degradation," *IEEE Trans. Instrum. Meas.*, vol. 71, p. 3509411, 2019.

[34] Z. Ye and J. Yu "State-of-health estimation for lithium-ion batteries using domain adversarial transfer learning," *IEEE Trans. Power Electron.*, vol. 37, p. 3528, 2022.

[35] J. Lu, R. Xiong, J. Tian, C. Wang, and F. Sun "Deep learning to estimate lithium-ion battery state of health without additional degradation experiments," *Nat Commun*, vol. 14, p. 2760, 2023.

[36] G. Ma, S. Xu, T. Yang, Z. Du, L. Zhu, H. Ding, and Y. Yuan "A transfer learning-based method for personalized state of health estimation of lithium-ion batteries," *IEEE Trans. Neural Netw. Learn. Syst.*, vol. 35, pp. 759–769, 2024.

[37] Z. Deng, L. Xu, H. Liu, X. Hu, B. Wang, and J. Zhou "Rapid health estimation of in-service battery packs based on limited labels and domain adaptation," *J. Energy Chem.*, vol. 89, pp. 345–354, 2024.

[38] S. Su, W. Li, J. Mou, A. Garg, L. Gao, and J. Liu "A hybrid battery equivalent circuit model, deep learning, and transfer learning for battery state monitoring," *IEEE Trans. Transp. Electrif.*, vol. 9, pp. 1113–1127, 2022.

[39] W. Zhang, J. Hu, B. Lin, D. Liu, M. Wang, D. Mu, and Y. Lu "Cross-domain state-of-health estimation of Li-ion batteries based on trasfer neural network with soft-dynamic time warping," *Energy Sci. Eng.*, vol. 11, pp. 3137–3148, 2023.

[40] J. Gotz, J. Galvao, F. Correa, A. Badin, H. Siqueira, E. Viana, A. Converti, and M. Borsato "Random forest-based grouping for accurate SOH estimation in second-life batteries," *Veh.*, vol. 6, pp. 799–813, 2024.

[41] E. Braco, I. Martin, P. Sanchis, A. Ursua, and D. Stroe "State of health estimation of second-life lithium-ion batteries under real profile operation," *Appl. Energy*, vol. 326, p. 119992, 2022.

[42] M. Faraji-Niri, M. Rashid, J. Sansom, M. Sheikh, D. Widanage, and J. Marco "Accelerated state of health estimation of second life lithium-ion batteries via electrochemical impedance spectroscopy tests and machine learning techniques," *J. Storage Mater.*, vol. 58, p. 106295, 2023.

[43] K. Severson, P. Attia, N. Jin, N. Perkins, B. Jiang, Z. Yang, M. Chen, M. Aykol, P. Herring, D. Fraggedakis, M. Bazant, S. Harris, W. Chueh, and R. Braatz "Data-driven prediction of battery cycle life before capacity degradation," *Nat. Energy*, vol. 4, pp. 383–391, 2019.

[44] Y. Zhang, M. Zhang, C. Liu, Z. Feng, and Y. Xu "Reliability enhancement of state of health assessment model of lithium-ion battery considering the uncertainty with quantile distribution of deep features," *Reliab. Eng. Syst. Saf.*, vol. 245, p. 110002, 2024.